Study of UV Cure Kinetics Resulting from a Changing Concentration of Mobile and Trapped Radicals

Yuemei Zhang,[†] David E. Kranbuehl,*[,†] Henry Sautereau,[‡] Gerard Seytre,[‡] and Jerome Dupuy[‡]

Department of Chemistry and Applied Science, College of William and Mary, Williamsburg, Virginia 23187, Université de Lyon, Lyon, F-69003, France, Université Lyon 1, IMP/LMPB Laboratoire des Matériaux Polyméres et Biomatériaux, Villeurbanne, F-69622, France, INSA de Lyon, IMP/LMM Laboratoire des Matériaux Macromoléculaires, Villeurbanne, F-69621, France, and CNRS, UMR5223, Ingénierie des Matériaux Polyméres, Villeurbanne, F-69621, France

Received September 20, 2007; Revised Manuscript Received November 16, 2007

ABSTRACT: UV cure kinetics of the system bisphenol A dimethacrylate and a phenylphosphine oxide initiator are studied as a function of incident intensity (I) and initiator concentration (PI). The rate of polymerization, $d(\ln[M(t)])/dt$, is found to be proportional to the intensity and initiator concentration raised to an exponential power of approximately 0.7 rather than the classical value of 0.5. The system does not obey classical steady-state kinetics but rather the rate of the reaction reaches a maximum shortly after gel and then decreases rapidly well before the reaction is quenched during the glass transition. These nonclassical results are proposed to be due to the coexistence of a varying ratio of the traditional bimolecular kinetics and a unimolecular trapped radical termination process due to the changing spatial/ dynamic heterogeneity arising from microgel formation in these systems. A model which focuses on the changing concentration of mobile active radicals is proposed. It uses four fitting parameters to describe changes in the total number of radicals minus the number of trapped immobile radicals. The model assumes a constant propagation rate constant, k_p, as is generally assumed in traditional crosslinking reactions up to the reaction quench in the final stage of the cure. The model is similar in mathematical form to a more complex multiparameter free volume molecular approach in which both k_p, k_t, and a trapping rate constant change with reaction advancement. Our model is based on the changing mobile radical concentration, which reflects the changes in the spatial heterogeneity of these systems due to the formation of microgels at the beginning of the reaction. It predicts the initial rapid buildup of the total radical concentration to a constant value and then the existence of an increasing proportion of trapped radicals up to reaction quenching in the glass transition. It accurately describes the UV cure kinetics at varying incident intensities and varying initiator concentrations and its predictions of the changes in the total and trapped radical concentrations are similar to ESR measurements on other systems.

Introduction

UV curing is well-known for its fast curing, energy saving, and environmental friendly advantages. Originally, it was mainly used in the coating industry for producing varnishes and inks. Today, UV curable material is not limited to the coating industry. It has found new applications in many other fields, such as encapsulates for microelectronic devices,[1] glass fiber and silica-filled polymer composites,[2] adhesives, stereolithography,[3−5] and dental restorative materials.[6−8]

Although UV curing technology has been widely used in industry, the reaction mechanism and kinetics are quite complex as the system moves quickly from a monomer mixture to a sol−gel and then is quenched during the glass transition.

The general kinetics and mechanism of free radical chain polymerization and photocure has been well reviewed.[9] The classic text book equation, eq 1, is derived based on the assumption of a steady-state concentration of active free radicals and a bimolecular termination.

$$-\frac{1}{[M]}\frac{d[M]}{dt} = -\frac{d(\ln[M])}{dt} = k_p\left(\frac{2.3\phi\epsilon I_i[PI]b}{k_t}\right)^{1/2} \quad (1)$$

where k_p and k_t are rate constants of propagation and termination, ϕ is quantum yield of initiation, ϵ is the extinction coefficient of initiator, [M] is the concentration of monomer, [PI] is the concentration of photoinitiator, b is the thickness of the sample, I_i is the incident light intensity. This equation shows that the cure rate is a function of intensity, photoinitiator concentration, and the sample thickness. k_p, k_t, ϕ, and ϵ are usually regarded as constants. It is also well-known that the cure rate is also a function of conversion[10−18] particularly at the gel point where the reaction auto accelerates. In order to explain this phenomena at the gel, a diffusion controlled termination mechanism was proposed and became very popular.[17−29] Diffusion controlled theory is based on bimolecular termination. It assumes that the radical does not terminate until it meets another radical. At the gel point, when the system viscosity increases significantly, it is much harder for a polymeric radical to diffuse and meet another radical. Therefore, the termination rate constant, k_t, is decreased by the decrease of the radical's diffusion ability and thereby the opportunity to meet another radical. In these models of divinyl polymerization, the mobility of monomers is not assumed to be affected significantly until quench during the glass transition, so the propagation rate, k_p, is not changed. Thus, in this respect, the system is viewed like most other crosslinking systems such as epoxies where the elementary binary rate constants remain unchanged until well into the final few percent of cure in the glass transition.[29] From eq 1, the total cure rate increases due to a decreased value of k_t. Although this approach

* To whom correspondence should be addressed.
[†] College of William and Mary.
[‡] Université de Lyon, Université Lyon 1, INSA de Lyon, and CNRS, UMR5223.

10.1021/ma702117e CCC: $40.75
Published on Web 12/29/2007

involving a changing k_t explains auto acceleration, it does not account for the deviation of the exponent from 0.5, a phenomena that has been observed in many reports.[10−18,30]

On the other hand, other authors have discussed the complex cure kinetics on conversion and the question of diffusion control of the propagation rate constant throughout the reaction. Soh and Sandburg argue that the translational movement of macroradicals becomes increasingly difficult, and segmental motion resulting from the propagation reaction becomes the prevailing mechanism.[20] Martin and Hamielec assume k_p remains constant up to a critical value of the free volume.[31] Stickler suggests that propagation is not diffusion but chemically controlled at low conversions and finds that the literature reports a wide range of results where k_p remains unchanged up to 50% conversion but in some cases a decrease occurs shortly after onset of the reaction.[19] Stickler's model uses only a single adjustable parameter, a critical free volume, which controls the onset of diffusion control. Russell, Napper, and Gilbert, and in several papers by Cook et al., build on these earlier works and assume k_p is constant for almost all of the reaction, and the overall reaction kinetics are determined by the transition from translation to reaction diffusion termination.[17,18,21]

Previously, it has also been noted by Bellobono et al. and by Cook that the exponent rose from 0.5 at low conversions to higher values approaching unity for a wide range of systems.[18,30] They proposed that this is due to the presence of first-order termination kinetics. This was suggested to be due to reaction of the radical with trace impurities or immobilization of the radical in the matrix.

These results were joined by a number of papers which focus on the existence and role of immobile, trapped radicals on the cure kinetics.[15,30−39] Bowman and co-workers have used ESR to monitor the rapid buildup in radicals after gelation and the fraction of trapped radicals versus conversion.[15,32,38] This was joined by Wen and McCormick's publication of a kinetic model describing the effects of radical trapping which builds on Bowman and co-workers' work.[39] Their model involves both a free volume diffusion controlled k_p, k_t, and a rate constant for radical trapping all of which are changing with free volume as the reaction advances. Their detailed fundamental kinetic model utilizes thirteen molecular parameters determined independently by experiment and/or from the literature plus six fitting parameters. For the system they studied, their model describes changes in the active radical concentration with conversion and that a higher light intensity leads to a lower fraction of trapped radicals at a given conversion and thereby a higher final conversion.

Over the past 10 years, additional insight into the changing morphology of these complex dimethacrylate systems is the verification of microgel formation at the onset of the cure reaction.[15,38,40] The hypothesis of a spatial heterogeneity was initially proposed by Ducek at al.[41−43] The existence of a spatial heterogeneity has led to verification of a dynamic heterogeneity through dielectric, dynamic mechanical, and DSC measurements which show an increasingly very broad glass transition with conversion.[44,45] These results and those of many others demonstrate that there exists simultaneously, beginning with the earliest stages of the reaction, regions of high molecular mobility sometimes referred to as liquid-like/monomer pool regions and regions of very low-molecular mobility in the growing micro/macrogel regions.

Here we report the results of experiments and a model which emphasizes the consequences of this changing spatial/dynamic heterogeneous polymerization environment. The model focuses on changes in the total concentration of radicals and the concentration of trapped radicals due to growth of the microgel regions. The kinetics and the effect of the UV intensity and the initiator concentration dependence on the cure kinetics are examined. The experiments reported on this paper are different from other published reports[46−50] in several aspects. First, the samples used in this paper have a thickness of 0.05 mm, and the initiator concentration is less than 0.2 wt %. Thereby, the total absorption of light through depth is less than 4% and the reaction can be regarded as homogeneous through depth. This is important as the results can be used to make accurate predictions of the cure kinetics versus depth in a thick sample. Second, the system is put between two pieces of glass like a sandwich so that the oxygen cannot diffuse into the sample during the curing process and the only oxygen that affects the cure is that initially dissolved in the system. Third, the cure intensity is less than 32.5 μW/cm^2, which is smaller than what was usually used in other reports. A water filter eliminates IR heating. Therefore, the cure rate is not fast and gives enough time for the reaction heat to release to the environment so that the cure is not affected by an increase of sample temperature. The results are then fit to an approach model which focuses on describing the changing proportion of active (mobile) and trapped (inactive) radicals while keeping k_p constant.

Experimental Section

Materials. The photoinitiator bis(2,4,6-trimethy-benzoyl)phenylphosphine oxide (Irgacure 819, Ciba) was dissolved in the pure oligomer, ethoxylated (4) bisphenol A dimethacrylate (CD540, Sartomer), molecular weight 540 with 100 ppm inhibitor. The system was stirred at room temperature for 1 h. The initiator concentration in the system is 0.05−0.2 wt %. All materials were used as received.

FTIR Analysis. In real-time, near FTIR measurements, with a FTS 7000 series FTIR spectrometer (Digilab), are used to measure the transmitted spectrum of the thin samples. The near FTIR spectrum monitors the decrease of the absorption peak (6160 cm^{-1}) area of the carbon double bonds of the oligomer during the cure process and thereby provides the conversion vs cure time profiles. The sample was prepared by putting it between two glass slides (transmission of IR > 95%, transmission of UV at 365 nm > 90%) using 0.05 mm Kapton tape as the spacer to determine the sample thickness.

The radiation source (200 W Hg lamp) has a 356−365 nm bandpass filter and is equipped with a water filter to remove the IR radiation's sample heating. A fiber optic cable guides the light to the sample chamber of the FTIR equipment. The intensity of the exposure is adjusted by changing the distance of the fiber optic cable from the sample.

Results

Light Intensity Effect on the Cure Kinetics of Thin Samples. A series of thin samples with the composition of CD540-0.2% Irgacure 819 were cured at various intensities from 32.5 to 1 μW/cm^2. The thickness of all the samples is 0.05 mm. The resulting conversion versus time monitored by real-time near FTIR is shown in Figure 1.

Figure 1 shows a delay period due to oxygen inhibition. This inhibition period is a function of the incident light intensity. After the oxygen in the system is consumed, the polymerization starts. The slope of the curves in Figure 1 represents the polymerization rate at different intensities. The slope is steep and then it levels off before the conversion of C═C reaches completion. The cure rate increases rapidly initially and then slows down, becoming extremely slow. The cure rate is a

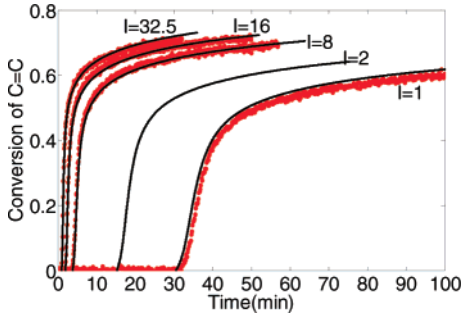

Figure 1. UV cure of CD540 with 0.2% Irgacure 819 at different intensities from 32.5, 16, 8, and 1 μW/cm^2. Calculation of cure conversion at different times for different intensities. (—) the calculated data, (• • •) the experimental data.

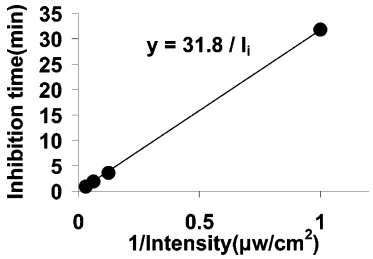

Figure 2. Delay time as a function of intensity at 32.5, 16, 8, and 1 μW/cm^2. CD540-0.2wt%IC819, thickness = 0.05 mm.

function of light intensity as the initial slope decreases with a decrease in light intensity.

Cure termination is due to the onset of the glassy state throughout the system. The final conversion is affected by the incident light intensity. Figure 1 shows that at the lower intensity, the reaction rate starts to slow down at a relatively low conversion. This has been explained by volume relaxation theory and radical trapping.[39,51]

In order to study quantitatively the effect of light intensity on the inhibition period, the inhibition time versus the value of 1/intensity is plotted in Figure 2. This figure shows that the delay time (in min) is inversely proportional to the incident intensity (in μW/cm^2) due to the presence of oxygen and the radical scavenger/stabilizer as previously shown by Wight and others[50−52] in eq 2.

$$T_d = \frac{31.8}{\text{Intensity}} \tag{2}$$

In Wight's paper, plots of delay time versus $1/I$ produced straight lines. The difference is that Wight found extrapolating those straight lines back to $1/I = 0$ gave nonzero values for the delay time. This is because the sample in that paper was exposed to the air. Therefore, oxygen could diffuse into the sample during the polymerization process to change the total amount of the oxygen which is scavenged by initiator radicals in the system. However, the concentration of the oxygen in the sample here can be regarded as a constant because there is no diffusion of oxygen as discussed above. In our case, extrapolating the lines back to $1/I = 0$ gives a zero value for the delay time.

In order to study the effect of incident light intensity on the polymerization rate of thin samples, the value of $-\mathrm{d}(\ln[\mathrm{M}(t)])/\mathrm{d}t$ as a function of conversion at different intensities is calculated using a 0.32 time interval and the result is shown in Figure 3.

In order to generate values of $-\mathrm{d}(\ln[\mathrm{M}(t)])/\mathrm{d}t$ with less experimental error at different conversions, the experimental data are fit to a polynomial curve using Excel software. Figure 3 shows that the solid fitted curves of $-\mathrm{d}(\ln[\mathrm{M}(t)])/\mathrm{d}t$ versus

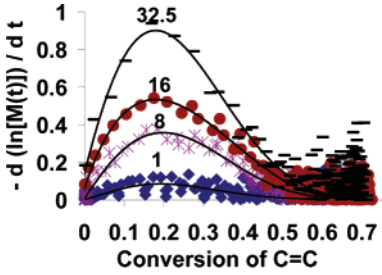

Figure 3. $-\mathrm{d}(\ln[\mathrm{M}(t)])/\mathrm{d}t$ versus conversion at different intensities at 32.5, 16, 8, and 1 μW/cm^2. CD540-0.2wt%IC819, thickness = 0.05 mm. ● are experimental data; — are the polynomial curve fitting results.

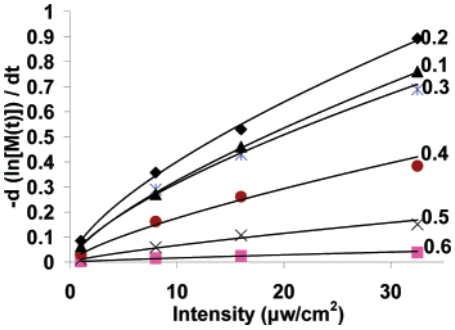

Figure 4. $-\mathrm{d}(\ln[\mathrm{M}(t)])/\mathrm{d}t$ versus intensity at different conversions (0.1−0.6). CD540-0.2wt%IC819, I_i = 32.5 μW/cm^2, thickness = 0.05 mm.

conversion of C═C at different intensities exhibit similar behavior. All four reactions experience at a low conversion an auto-acceleration process that is known as the Trommsdorff or gel effect. After the conversion of C═C reaches about 18%, the reaction rate starts to drop. The reason for the increase and decrease of the reaction rate over the range of conversion to 50% can be explained as previously reported by assuming a changing total concentration of radicals and that some become trapped in the growing microgel regions. The value of $-\mathrm{d}(\ln[\mathrm{M}(t)])/\mathrm{d}t$ at conversions from 0.1 to 0.6 are determined at different intensities from the solid curves in Figure 3. In the region of 0.5−0.6, the reaction is quenched as the glass transition is approached throughout the sample. In this region as k_p is rapidly reduced due to dramatic changes in mobility, only a small amount of additional reaction occurs.

Plots of $-\mathrm{d}(\ln[\mathrm{M}(t)])/\mathrm{d}t$ versus intensity at different conversions are shown in Figure 4.

From Figure 4, it is found that the relationship of $-\mathrm{d}(\ln[\mathrm{M}(t)])/\mathrm{d}t$ to intensity is fit at different degrees of conversion by

$$\frac{\mathrm{d}(\ln[\mathrm{M}(t)])}{\mathrm{d}t} \propto a\text{Intensity}^b \tag{3}$$

As seen in Table 1, the value of b is 0.70 ± 0.04 for the conversion range from 10% to 50%. After 50% conversion, the value of b increases considerably. Comparison of the b value here with the value of the exponent in eq 1, it is found that b is higher than the classic value, 0.5. We attribute this to unimolecular termination which is occurring due to trapping of a portion of the radicals in the microgel regions. As described, trapped radicals have been extensively observed in many free radical polymerization systems.[15,25,28,32,36−38,52,53] These immobile radicals can terminate themselves by a unimolecular mechanism and in this case the cure kinetics can be expressed by eq 1, where the value of the exponent is equal to 1. Thus the value of b approaches 0.5 if bimolecular termination is the

Table 1. The Values of *a* and *b* in Equation 3 at Different Degrees of Conversion[a]

conversion of C=C	$a \times 1000$	b
0.1	62.1	0.72
0.2	85.2	0.67
0.3	64.6	0.69
0.4	31.9	0.74
0.5	10.9	0.78
0.6	2.5	0.82

[a] Here the consumption of initiator is not been considered in this section because it is less than 1.2% for all the systems studied here when the conversion of C=C is less than 50%.

main termination process, and it approaches 1 if unimolecular termination is the main process. The values of b between 0.5 and 1.0 reported in Table 1 support the existence of both mobile and trapped radicals throughout the cure process. The increase in the value of b considerably beyond 0.7 at a conversion greater than 50% reflects the onset of the glass transition region and extensive radical trapping throughout the system as the viscosity rapidly increases during the glass transition.[15,32,38]

In the glass transition region, Bowman and co-workers[32,38] found the concentration of trapped radicals to be almost equal to the total radical concentration. From eqs 1 and 3, many more trapped radicals in the system means more unimolecular termination relative to bimolecular termination which correlates with the value of b approaching 1.

Modeling Polymerization Rate Versus Conversion at One Intensity. A model is developed to fit the experimental curve of $-\mathrm{d}(\ln[\mathrm{M}(t)])/\mathrm{d}t$ versus conversion at the intensity of 32.5 μw/cm^2 in Figure 3 up to a conversion of 0.5. The existence of a changing concentration of trapped radicals in the growing micro/macrogel regions and a constant value of k_p is used as the theoretical basis for the model. In the model, the radicals in the system are divided into two groups, completely "free/mobile" radicals and completely "trapped/immobile" radicals. The reaction rate constant, k_p, of "free" radicals is considered unchanged, as commonly assumed in most crosslinking reactions. On the other hand, "trapped" radicals are considered completely immobile, enclosed by the growing micro/macrogel network and have no chance to react with another radical. Thus in the model, at any point in time, radicals are assumed to be in one of two extreme situations reflecting the mobile and immobile regions in these systems. Thus the radicals can be divided into a percent of completely "free/mobile" radicals and a percent of completely "trapped/immobile" radicals which reflects the changes into spatial and dynamic heterogeneity during the course of the reaction. According to this description, we can write an equation for the reaction of a radical with a monomer

$$-\frac{1}{[\mathrm{M}(t)]}\frac{\mathrm{d}[\mathrm{M}(t)]}{\mathrm{d}t} = -\frac{\mathrm{d}(\ln[\mathrm{M}(t)])}{\mathrm{d}t} = k_p[\mathrm{M}_f^{\bullet}] \qquad (4)$$

The changing value of $-\mathrm{d}(\ln[\mathrm{M}(t)])/\mathrm{d}t$ versus conversion in Figure 3 is due to the value of k_p times the changing value of $[\mathrm{M}_f^{\bullet}]$, the free radical concentration. Here k_p remains a constant that does not change with conversion until the reaction is quenched during the glass transition. The concentration of free radicals is equal to the changing total concentration of radicals minus those that are trapped.

$$[\mathrm{M}_f^{\bullet}] = [\mathrm{M}^{\bullet}]_{total} - [\mathrm{M}_t^{\bullet}] \qquad (5)$$

and eq 4 can be rewritten as

$$-\frac{\mathrm{d}(\ln[\mathrm{M}(t)])}{\mathrm{d}t} = k_p[\mathrm{M}^{\bullet}]_{total} - k_p[\mathrm{M}_t^{\bullet}] \qquad (6)$$

Using eq 6, the UV cure results for CD540-0.2wt%IC819 at intensity of 32.5 μW/cm^2 in Figure 3 are fit using eq 7, which is the difference of two reciprocal exponential expressions.

$$-\frac{\mathrm{d}(\ln([\mathrm{M}(t)]))}{\mathrm{d}t} = \frac{1}{1+\mathrm{e}^{-30(\alpha-0.05)}} - \frac{1}{1+\mathrm{e}^{-13.7(\alpha-0.36)}} \qquad (7)$$

Here α is the conversion of C=C. The first factor, $1/(1+\mathrm{e}^{-30(\alpha-0.05)})$, represents the contribution of k_p times $[\mathrm{M}^{\bullet}]_{total}$, the concentration of all radicals in the system. The second factor, $1/(1+\mathrm{e}^{-13.7(\alpha-0.36)})$, represents the contribution of k_p times $[\mathrm{M}^{\bullet}]_t$, the concentration of trapped radicals. The parameters of 30 and 13.7 times the extent of reaction α, describe the magnitude of k_p times the rate of increase in the concentration of total radicals and trapped radicals, respectively. The parameters 0.05 and 0.36 describe the value of the conversion, α, when the rapid rise in the concentration of total and trapped radicals occurs. They are the value of α when the total and trapped radical concentration is equal to half of their maximum.

The mathematical expressions in eq 7 are a Sigmoid function, an equation that describes well the rapid increase and the subsequent slow decrease in some polymer properties. One example is the sudden rapid change in tensile properties versus molecular weight during the ductile−brittle transition common to most semicrystalline thermoplastics.

Similar kinetic Sigmoid type equations for propagation, termination, and trapping were developed in the diffusion control approach based on changes in the free volume during the reaction in the paper by Wen and McCormick.[39] In their derivation they use the free volume dependence of k_p, k_t, and a trapping rate constant to reflect the consequences of changes in the spatial heterogeneity as the reaction advances. As such their free volume dependence is an average free volume reflecting the dynamics of what we consider to be two extremes; the mobile fluidlike low-molecular weight regions and the immobile-trapping regions of the growing micro/macrogel regions. We suggest that such an average is better suited to a homogeneous system where time/spacial averaging is appropriate. Their final kinetic expression for predicting the reaction rate involves 19 parameters, of which 13 are measurable molecular parameters characterizing a particular polymer system, while others are adjustable to fit the shape of the overall reaction.

This is in contrast to our approach which uses far fewer fitting parameters and which is completely different as it focuses on the effect of having a widely varying heterogeneity of a loosely to densely crosslinked network structure. This fact suggests that an approach for modeling the kinetics should emphasize the changing concentration of mobile and trapped radicals as the reaction progresses.

Here we assume, as in most crosslinking reactions, that k_p is an approximate constant for almost all of the reaction, that is until the final stage where the reaction rate is quite small and the final few additional percent of conversion occurs during quenching of the entire reaction while in the glass transition region. In eq 7 as described there are four additional parameters to describe the changes in the concentration versus conversion of the total number of radicals and of the trapped radicals. Thus, the focus is on the changing concentration of mobile, free radicals times a constant propagation rate constant up until the onset of the glass transition at $\alpha > 0.5$. This approach emphasizes the effect of the changing heteroge-

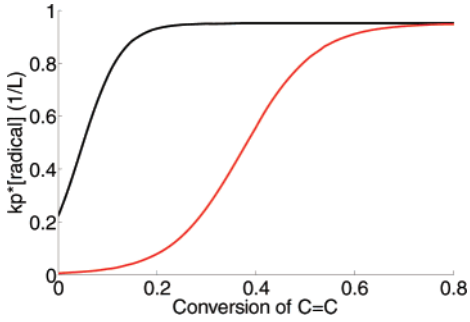

Figure 5. The model's predicted concentration of total radicals and trapped radicals versus conversion for the cure of a sample, CD540-0.2wt%Irgacure 819, at room temperature under intensity of 32.5 μW/cm^2, thickness = 0.05 mm. (—) the total radical concentration, (– – –) the trapped radical concentration.

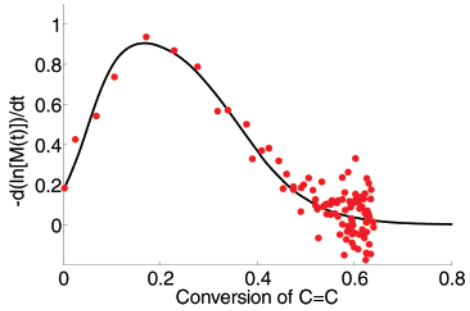

Figure 6. −d(ln[M(t)])/dt versus conversion at room temperature under an intensity of 32.5 μW/cm^2, CD540-0.2wt%Irgacure 819, thickness = 0.05 mm. (●) the experimental data, (—) the model predicted values.

neous spatial morphology of dimethacrylate systems where the fraction of immobile micro/macrogel regions increases from the beginning of the reaction to the reaction quench in the glass transition.

Using eq 7, the changing concentration of total radicals and "trapped" radicals is shown in Figure 5. From Figure 5, the model predicts that the concentration of total radicals in the system increases very fast at the beginning. After 20% conversion, total radical concentration becomes constant. The model predicts that the fraction of trapped radicals is low when the conversion is less than 20%; however after that, the fraction of trapped radicals increases significantly till 50% conversion. After 50% in the glass formation region, most of the radicals in the system are trapped radicals. These predictions using the model as applied to the dimethacrylate system studied here are quite similar to those observed on another system using ESR measurements by Bowman and co-workers.[32,38]

The model predicts a leveling off to a constant value of the total radical concentration. This is in contrast to experimental results which show a gradual continual increase for another system as it remains rubbery but approaches the glass transition region. The experimental results show that the rate of the gradual increase as opposed to a leveling off to a constant value is correlated with the fraction of highly crosslinked regions that are already glassy during the course of the polymerization. Since these radicals are trapped in the glassy region and the vast majority of the cure occurs well before reaction quenching in this region, the model and its predicted leveling based on the changing concentration of mobile radicals accurately describes the reaction rate up to reaction quench in the glass transition region.

Using eq 7, in Figure 6 the model predictions are compared with the experimental data of −d(ln[M(t)])/dt versus conversion

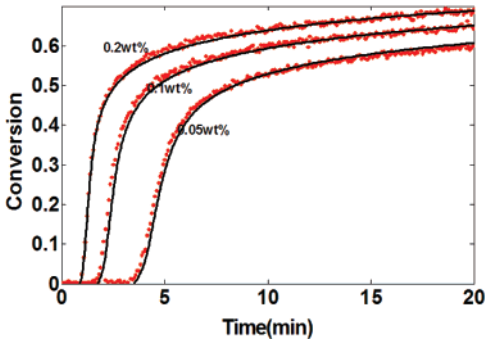

Figure 7. UV cure of C═C conversion with varying concentrations of Irgacure 819 of 0.2%, 0.1%, and 0.05%; I = 32.5 μW/cm^2. Model predicted values of C═C conversion versus time for different [PI], photoinitiator concentration. (—) the calculated data, (• • •) the experimental data

for the intensity of 32.5 μW/cm^2. Figure 6 shows that the model calculated curve fits the experimental data well over the entire range of conversion. Thus eq 7 can be used to predict −d(ln[M(t)])/dt versus conversion for the cure of the system CD540-0.2 wt % Irgacure 819 at room temperature, I_i = 32.5 μW/cm^2, thickness = 0.05 mm.

Prediction of UV Cure Kinetics at Different Intensities. Combining eqs 3 and 7, the value of −d(ln[M(t)])/dt versus conversion and time at other incident intensities (I_i) can be calculated using eq 8.

$$-\frac{\mathrm{d}(\ln([\mathrm{M}(t)]))}{\mathrm{d}t} = Af(\alpha) \qquad (8)$$

where f (α) is the right-hand side of eq 7, $A = (I_i/32.5)^{0.7}$, and the units of I_i are μW/cm^2.

The conversion of C═C, α, versus cure time is calculated for the cure of bisphenol A dimethacrylate with 0.2wt%IC819 at different light intensities using eq 8. Note that the cure times, t_1 to t_n, take the cure starting point at the end of the inhibition period, instead of the exposure starting point, as 0. The length of the inhibition period is calculated for any given intensity using eq 2 for the bisphenol A dimethacrylate the system with 0.2 wt % Irgacure 819 at room temperature with a thickness of 0.05 mm.

With the use of the method above, the cure kinetics of bisphenol A dimethacrylate 0.2wt%Irgacure 819 thin films at the different exposure intensities of 32.5, 16, 8, and 1 μW/cm^2 are calculated and the model predicted results are shown in Figure 1 as the solid curves. The experimental data are listed in the same figure as the dotted curves to compare with the predicted curves. Figure 1 shows that the predicted curves fit the experimental data very well. The outcome demonstrates that it is possible to predict the cure kinetics of a thick sample at different depths since the changing intensity versus depth and exposure time is the main reason for the change of cure kinetics in thick samples.

Initiator Concentration Effect on Cure Kinetics. A series of thin samples of bisphenol A dimethacrylate and Irgacure 819 at varying concentrations of 0.05 to 0.2 wt % were cured at the intensity of 32.5 μW/cm^2, thickness of 0.05 mm. The conversion of C═C versus exposure time is shown in Figure 7. The inhibition period, reaction rate, and the final conversion are all functions of initiator concentration, [PI], with a similar effect to increasing the light intensity as both directly affect the rate of formation of radicals.

The delay time versus the value of 1/[PI] is plotted in Figure 8. The delay time is longer for the system with less initiator

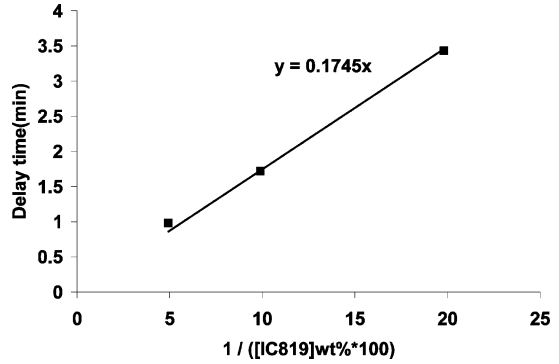

Figure 8. Delay time as a function of [PI], $I = 32.5\ \mu W/cm^2$.

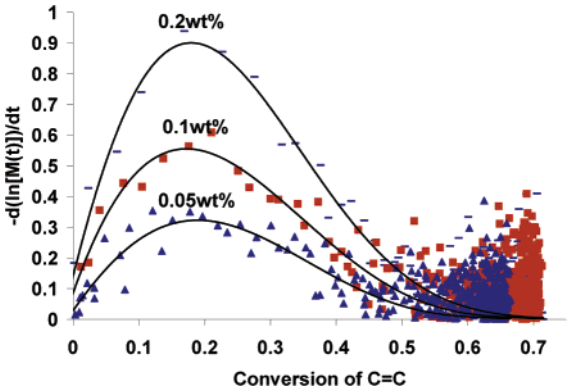

Figure 9. $-d(\ln[M(t)])/dt$ versus conversion for system with different initiator concentrations, [PI], $I_i = 32.5\ \mu W/cm^2$, thickness = 0.05 mm. Points are experimental data; solid curves are the fitting polynomials.

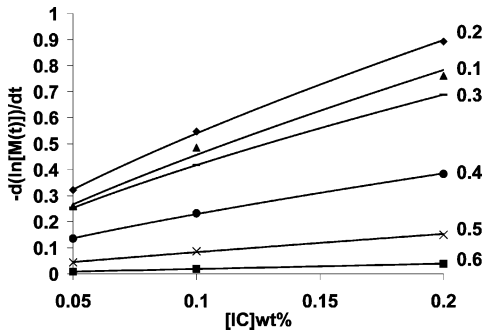

Figure 10. [PI] effect on the value of $-d(\ln[M(t)])/dt$ at different degrees of conversion (0.1−0.6 marked in the figure).

concentration as observed in Decker's paper[54] for the polymerization with much higher cure rate. Studying the relationship of delay time T_d (in min) and [PI] gives eq 9.

$$T_d = \frac{0.1745}{[\text{PI}]\text{wt \%} \times 100} \tag{9}$$

Figure 9 shows that increasing the initiator concentration results in a larger polymerization rate and final conversion. In order to study the connection between the polymerization rate and [PI], the value of $-d(\ln[M(t)])/dt$ versus conversion at various initiator concentrations is plotted in Figure 9.

Similar to Figure 3, the experimental data in Figure 9 are fit to curves using a polynomial and Excel software to give values of $-d(\ln[M(t)])/dt$ with less experimental error versus conversion. The value of $-d(\ln[M(t)])/dt$ versus [PI], the photoinitiator concentration at different conversions of C=C is shown in Figure 10.

Table 2. The Values of *c* and *d* in Equation 11 at Different Degrees of Conversion[a]

conversion of C=C	*c*	*d*
0.1	2.71	0.77
0.2	2.90	0.73
0.3	2.18	0.71
0.4	1.28	0.74
0.5	0.62	0.86
0.6	0.21	1.03

[a] The values are calculated using corrected initiator concentrations at different conversions.

From Figure 10, the relationship of $-d(\ln[M(t)])/dt$ and [PI] can be described as

$$-\frac{d(\ln[M(t)])}{dt} \propto c[\text{PI}]^d \tag{10}$$

In Table 2, the value of d (0.75 ± 0.04) is almost a constant for the conversion range from 10% to 40% where the reaction rate is large. This value is within the experimental error of the value of b, 0.7 in eq 3. As before, the deviation of the value of b and d from 0.5 is attributed to the unimolecular termination kinetics due to trapped radicals in the system whose concentration rapidly increases around a conversion of 0.5. When the conversion of C=C reaches 0.5, d increases to 0.88. At 0.6 conversion it becomes essentially 1 when the percentage of trapped radicals rapidly increases as the reaction is quenched when the system enters the glass transition region.

Prediction of UV Cure Kinetics at Different Initiator Concentrations. From eq 10 and the previous eqs 7 and 9, the cure kinetics of bisphenol A dimethacrylate with different initiator concentrations, [PI], at 32.5 $\mu W/cm^2$ intensity can be calculated. The model's predicted results are shown in Figure 7.

Given the good fit, the cure kinetics of a thin sample of bisphenol A dimethacrylate with Irgacure 819 at varying Irgacure 819 concentrations and varying the radiation intensity can be described by combining eqs 2 and 9 to give eq 11,

$$T_d = \frac{5.542}{I[\text{PI}]\text{wt \%} \times 100} \tag{11}$$

This reciprocal dependence of induction time is known to reflect the presence of oxygen as a radical scavenger and/or of added stabilizer.[55,56]

Combining eqs 7, 8, and 10 gives eq 12,

$$\left(-\frac{d(\ln[M(t)])}{dt}\right)_{I_2, \text{PI}_2} = K\left(\frac{I_2}{I_1}\right)^b\left(\frac{\text{PI}_2}{\text{PI}_1}\right)^d \tag{12}$$

Here K is described by eq 7 for $I_1 = 0.32\ \mu W/cm^2$ and $[\text{PI}]_2 = 0.2$ wt % while b is 0.70 and d is 0.75 for this system.

Equation 12 utilizes a fit at one intensity and initiator concentration to describe the changes in the rate of polymerization versus the changing total concentration of radicals and concentration of trapped radicals. This rate dependent eq 7 is then scaled to other intensities and initiator contractions based on the independently determined exponential parameter b for intensity and d for initiator concentration which for this system are about 0.7. The value 0.7 reflects the combination of unimolecular and bimolecular termination which is occurring up to the reaction quench in the glass transition.

With eqs 11 and 12, the cure kinetics of bisphenol A dimethacrylate with Irgacure 819 can be predicted as a function

of UV intensity I_2 and the amount of initiator concentration $[PI]_2$ when the sample thickness is small.

This equation emphasizes the spatial heterogeneity due to the growing micro/macrogel regions throughout the reaction and the resulting changes in the concentration of the total radical concentration minus the trapped radical concentration. It assumes a constant k_p. It describes the I and PI dependence for almost all of the reaction. After 50% conversion, the reaction rate is very small and the reaction advances only a small amount during diffusion controlled quenching of now a changing k_p in the glass transition.

Conclusions

As previously shown, UV cure kinetics of this dimethacrylate system composed of bisphenol A dimethacrylate and a phenylphosphine oxide initiator are a function of incident intensity and initiator concentration. The inhibition period of the free radical photopolymerization due to the existence of previously dissolved oxygen is inversely proportional to the initiator concentration and the incident intensity with an intercept of zero if no further oxygen is allowed to diffuse into the sample.

The rate of polymerization, $d(\ln[M(t)])/dt$, is found proportional to the intensity and initiator concentration raised to an exponential power of approximately 0.7 rather than the classical value of 0.5. The increase of the exponential value from the theoretical value of 0.5 in eq 1 is proposed to be due to unimolecular termination of "trapped" radicals as observed previously by ESR spectra.

The existence of a changing concentration of trapped radicals in the growing micro/macrogel regions and a constant value of k_p is used as the basis for the model. In the model, the radicals in the system are divided into two groups, completely "free/mobile" radicals and completely "trapped/immobile" radicals. "Trapped" radicals are considered completely immobile, enclosed by the growing micro/macrogel network and have no chance to react with another radical. Thus at any point in time, radicals are assumed to be in one of two extreme situations and are divided into "free/mobile" radicals and completely "trapped" radicals reflecting the changes in the spatial/dynamic heterogeneity resulting from the growing micro/macrogel regions throughout the reaction.

Four parameters in two exponential functions are used to describe k_p time changes in the total number of radicals minus the number of trapped immobile radicals where the propagation rate constant, k_p, is approximated as constant up to the reaction quench in the final stage of the cure. The model is similar in mathematical form to a more complex multiparameter free volume molecular approach in which both k_p, k_t, and a trapping rate constant change with reaction advancement.

Our model predicts the initial rapid buildup of the total radical concentration to a constant value, the steady state approximation, and then the existence of an increasing proportion of trapped radicals up to reaction quenching in the glass transition. The model's predictions of the changes in the trapped radical concentration are in good agreement with ESR results in other dimethacrylate systems. The model accurately describes the UV cure kinetics at varying incident intensities and varying initiator concentrations.

The results offer a method to study the cure kinetics of dimethacrylate systems in which the changing concentration of free/mobile and trapped/immobile radicals represents the changes in the spatial/dynamic heterogeneity due to growth of micro/macrogel regions throughout the reaction.

References and Notes

(1) Baikerikar, K. K.; Scranton, A. B. *Polymer* **2001**, *42*, 431−441.
(2) Sipani, V.; Coons, L. S.; Rangarajan, B.; Scranton, A. B. Photopolymerization of Composites: Recent Developments in Glass-Fiber and Silica-Filled Systems. In *RadTech Report 2003 A Year in Review*; RadTech International North America: Bethesda, MD, 2003; pp 22−26.
(3) Lee, J. H.; Prudhomme, R. K.; Aksay, I. A. *J. Mater. Res.* **2001**, *16*, 3536−3544.
(4) Decker, C.; Elzaouk, B. *J. Appl. Polym. Sci.* **1997**, *65*, 833−844.
(5) Decker, C. *Nucl. Instrum. Methods Phys. Res., Sect. B* **1999**, *151*, 22−28.
(6) Lovell, L. G.; Berchtold, K. A.; Elliott, J. E.; Lu, H.; Bowman, C. N. *Polym. Adv. Technol.* **2001**, *12*, 335−345.
(7) Elliott, J. E.; Lovell, L. G.; Bowman, C. N. *Dent. Mater.* **2001**, *17*, 221−229.
(8) Lovell, L. G.; Stansbury, J. W.; Syrpes, D. C.; Bowman, C. N. *Macromolecules* **1999**, *32*, 3913−3921.
(9) Odian, G. *Principles Of Polymerization*, 3rd ed.; John Wiley & Sons, Inc.: New York, 1991.
(10) Berchtold, K. A.; Lovestead, T. M.; Bowman, C. N. *Macromolecules* **2002**, *35*, 7968−7975.
(11) Andrzejewska, E. *Prog. Polym. Sci.* **2001**, *26*, 605−665.
(12) Tryson, G. R.; Shutz, A. R. *J. Polym. Sci., Part B: Polym. Phys.* **1979**, *17*, 2059−2075.
(13) Kloosterboer, J. G.; Lijten, G. F. C. M. *Polym. Commun.* **1987**, *28*, 2−5.
(14) Decker, C.; Bendaikha, T. *Makromol. Chem.* **1988**, *189*, 2381−2394.
(15) Lovestead, T. M.; Berchtold, K. A.; Bowman, C. N. *Macromolecules* **2005**, *38*, 6374−6381.
(16) Scherzer, T.; Decker, U. *Radiat. Phys. Chem.* **1999**, *55*, 615−619.
(17) Cook, W. D. *J. Polym. Sci., Part A: Polym. Chem.* **1993**, *31*, 1053−1067.
(18) Cook, W. D. *Polymer* **1992**, *33*, 2152−2161.
(19) Stickler, M. *Macromol. Chem.* **1988**, *184*, 2563−2579.
(20) Soh, S.; Sundberg, D.C. *J. Polym. Sci.* **1982**, *20*, 1299−1329.
(21) Russell, G.; Naper, D.; Gilbert, R. *Macromolecules* **1998**, *21*, 2133−2140.
(22) Young, J. S.; Bowman, C. N. *Macromolecules* **1999**, *32*, 6073−6081.
(23) Terrones, G.; Pearlstein, A. J. *Macromolecules* **2004**, *37*, 1565−1575.
(24) Benson, S. W.; North, A. M. *Kinetics of Free Radical Polymerization*; Pergamon Press: New York, 1962; p 935.
(25) Lovestead, T. M.; O'Bren, A. K.; Bowman, C. N. *J. Photochem. Photobiol. A: Chem.* **2003**, *159*, 135−143.
(26) Mateo, J. L.; Serrano, J.; Bosch, P. *Macromolecules* **1997**, *30*, 1285−1288.
(27) Hamielec, A. E. *Chem. Eng. Commun.* **1983**, *24*, 1−19.
(28) Anseth, K. S.; Wang, C. M.; Bowman, C. N. *Macromolecules* **1994**, *27*, 650−655.
(29) Pascault, J. P.; Sautereau, H.; Verdu, J.; Williams, R. J. J. *Themosetting Polymers*; Marcel-Dekker: New York, 2002.
(30) Bellobono, I. R.; Selli, E.; Righetto, L.; Rafellini; Trevisan, L. *Makromol. Chem.* **1989**, *190*, 1945.
(31) Martin, F. L.; Hamielee, A. E. *ACS Symp. Ser.* **1978**, *104*, 43.
(32) Berchtold, K. A.; Randolph, T. W.; Bowman, C. N. *Macromolecules* **2005**, *38*, 6954−6964.
(33) Kloosterboer, J. G.; Lijten, C. M.; Greidanus, F. J. A. *Polym. Rep.* **1986**, *27*, 268.
(34) Kloosterboer, J. G.; Van de Hei, G. M. M.; Boots, H. M. J. *Polym. Commun.* **1984**, *25*, 354−357.
(35) Kloosterboer, J. G.; Van de Hei, G. M. M.; Gossink, R. G.; Dortant, G. C. M. *Polym. Commun.* **1984**, *25*, 322−325.
(36) Zhu, S.; Tian, Y.; Hamielec, A.; Eaton, D. R. *Polymer* **1990**, *31*, 1726.
(37) Zhu, S.; Tian, Y.; Hamielec, A. E. *Macromolecules* **1990**, *23*, 1144−1150.
(38) Anseth, K. S.; Anderson, K. J.; Bowman, C. N. *Macromol. Chem. Phys.* **1996**, *3*, 833−846.
(39) Wen, M.; McCormick, A. V. *Macromolecules* **2000**, *33*, 9247−9254.
(40) Rey, L.; Galy, J.; Sautereau, H. *Macromolecules* **2000**, *33*, 6780−6786.
(41) Dusek, K. *Polym. Gels Networks* **1996**, *4*, 383−404.
(42) Dusek, K. *Angew. Makromol. Chem.* **1995**, *240*, 1−15.
(43) Dusek, K.; Matejka, L.; Spacek, P.; Winter, H. *Polymer* **1996**, *37*, 2233−2242.
(44) Guo, Z.; Sautereau, H.; Kranbuehl, D. E. *Polymer* **2005**, *46*, 12452−12459.
(45) Guo, Z.; Sautereau, H,; Kranbuehl, D. E. *Macromolecules* **2005**, *38*, 7992−7998.
(46) Chong, J. S. *J. Appl. Polym. Sci.* **1969**, *13*, 241−247.
(47) Studer, K.; Decker, C.; Bech, E.; Schwalm, R. *Prog. Org. Coat.* **2003**, *48*, 92−100.

(48) Studer, K.; Decker, C.; Bech, E.; Schwalm, R. *Prog. Org. Coat.* **2003**, *48*, 101−111.
(49) Decker, C.; Jenkins, A. D. *Macromolecules* **1985**, *18*, 1241−1244.
(50) Wight, F. R. *J. Polym. Sci., Polym. Lett. Ed.* **1978**, *16*, 121−127.
(51) Lecamp, L.; Youssef, B.; Bunel, C.; Lebady, P. *Polymer* **1999**, *40*, 6313−6320.
(52) Truffier-Boutry, D.; Gallez, X. A.; Demoustier-Champagne, S.; Devaux, J.; Mestdagh, M.; Champage, B.; Leloup, G. *J. Polym. Sci., Part A: Polym. Chem.* **2003**, *41*, 1691−1699.
(53) Hara, S.; Yamamoto, K.; Shimada, S.; Nishi, H. *Macromolecules* **2003**, *36*, 5661−5665.
(54) Decker, C.; Masson, F.; Keller, L. *Polym. Prepr.* **2003**, *88*, 215−216.
(55) Cook, W. D. *J. Appl. Polym. Sci.* **1991**, 2209−2228.
(56) Cook, W. D. *Polym. Int.* **2001**, 129−134.

MA702117E